© Universiti Tun Hussein Onn Malaysia Publisher's Office

**IJIE**

Journal homepage: http://penerbit.uthm.edu.my/ojs/index.php/ijie
ISSN : 2229-838X e-ISSN : 2600-7916

The International Journal of Integrated Engineering

# A Preliminary Study of Internal Corrosion in Condensate Pipelines at Geothermal Power Plants

**Ahmad Royani[1*], Siska Prifiharni[1], Gadang Priyotomo[1], Joko Triwardono[1], Sundjono[1]**

[1]Research Center for Metallurgy and Material – Indonesian Institute of Sciences, Puspiptek regions, 470 Buildings, South Tangerang-Banten 15314, INDONESIA

*Corresponding Author

DOI: https://doi.org/10.30880/ijie.2021.13.04.011
Received 22 April 2020; Accepted 30 March 2021; Available online 30 April 2021

**Abstract:** In this study, we presented observations and analyze related to internal corrosion in condensate pipes in geothermal power plants. A damaged pipe of condensate pipeline taken from a power plant was investigated to determine the root cause of failure. The observation and failure analysis was carried out by visual and dimensional examination, chemical composition testing, macroscopic, and microscopic examination, Scanning Electron Microscope (SEM) examination with Energy Dispersed Spectrometer (EDS). The deposit in the pipe was analyzed by X-Ray Diffraction (XRD). The quality of the condensate fluid and their tendencies were determined by Langelier Saturation Index (LSI). Also, the corrosion rate of the pipe was simulated by condensate fluid by using a corrosion measurement system (Tafel polarization). The internal corrosion was found in the condensate line is strongly suspected to occur due to erosion-corrosion. Erosion corrosion is caused by insoluble and hard particles in the condensate fluid. The results of XRD found the presence of calcium-silicate compounds in the sediment that is suspected to be the cause of erosion particles. The reduction of the thickness of the bottom pipe wall and occurs in longitudinal directions the alleged damage to the pipe due to sediment corrosion. The presence of hard compounds and differential oxygen can accelerate the process of corrosion so that the corrosion rate in condensate pipelines was a category in the severe category based on NACE SP0775 standards.

**Keywords:** Condensate line, erosion, failure analysis, internal corrosion, power plant

## 1. Introduction

Geothermal power generation is growing because of the need for clean renewable energy and environment-friendly power. The geothermal resources can generate continuous power at the lowest cost with minimum environmental impact. Indonesia is a leading country in terms of geothermal power plants and one of the countries that have a large potential of geothermal resources in the world [1]. In recent years, the Indonesian government has been strongly promoting expansions and development of the geothermal power plant aimed at a substitution of a certain part of the consumption of oil and other fossil fuels. Fouling mitigation and corrosion control are big challenges in developing geothermal energy [2].

Corrosion is a natural process through which metals in their manufactured or refined states return to their natural, more stable oxidation states [3]. This process is thought of as a redox reaction where the metal becomes oxidized because of exposure to oxygen. Three things are required for corrosion to occur: metal, oxygen, an electrolyte [3]. Scaling, or sometimes known as precipitation fouling, is the action by which there is the crystallization of solid salts and (hydro)oxides from solutions, usually that of water, or brine [4]. Scaling depends on three physical conditions: temperature, pressure, and pH [5]. These affect the minerals in solution, which then leads to scaling. Though pressure does not directly influence mineral solubility, it instead affects the gas solubility, which consequently affects the pH and

*Corresponding author: ahmad.royani@lipi.go.id

then the mineral solubility [5]. Corrosion and scaling can occur in the production wells, heat exchangers, boilers, pipelines, and injection wells [2].

Water has a large influence on the corrosion processes and the formation of scales. The water's chemical characteristics will influence the stability of water as well as affect the extent of corrosion and scaling processes [6]. The primary factors that affect both corrosion and scaling are water hardness, alkalinity, and pH, while oxidizing agents (such as carbon dioxide and dissolved solids) affect corrosion only [6-7]. Three primary factors (hardness, alkalinity, and pH) determine if the water produces scales, causes corrosion, or stable [7]. Water that has a more corrosive nature is indicated by low pH, low alkalinity, and soft (non-carbonate) hardness [7]. Water that is more scale forming in nature tends to have a high pH, hard (with carbonates) hardness, and high alkalinity [7]. Alkalinity measures how easily the pH of water can be changed. Hence, water with high alkalinity is more scale forming even with relatively low pH values, while low-alkalinity waters are not able to buffer against acids, thus, they are more corrosive [8]. The Langelier Saturation Index (LSI) is probably the most widely used indicator of the water scale potential. This index indicates the driving force for scale formation and and growth in terms of pH as a master variable [6]. To calculate the LSI index, it is necessary to know the calcium hardness (mg/L $Ca^{2+}$ as $CaCO_3$), the actual pH, the total dissolved solids (mg/L, TDS), the alkalinity (mg/L as $CaCO_3$ or calcite), and the temperature of the water ($^oC$) [6].

Other secondary chemical factors in water can affect corrosion and formation of scales are such as carbon dioxide and total dissolved solids (TDS). Carbon dioxide ($CO_2$) is the main gas affected by pressure change [5]. During the production of water from the reservoir, the pressures are significantly reduced as it reaches the surface [9]. This pressure reduction will cause the solubility of gas to decline, and consequently lead to degassing as the gas comes out of water. In turn, this increases the pH and lowers the solubility of many scales forming minerals. Carbon dioxide also leads to corrosion because the gas can combine with water to make acid (thought this could reduce scaling) which ends up in low pH and more acidic conditions. The total dissolved solids show what ions are in the water and if their number of ions be high then scaling is more likely. Furthermore, the greater number of ions will increase the electrical conductivity of the water thus increasing the rate of corrosion [10]. Other factors influencing corrosion is the temperature (also affects scaling) and flow velocity [11-12]. Both temperature and flow velocity have been a complex effect on the corrosion rate. The temperature has a mixed effect on scaling depending on whether it is a low or high temperature. High temperatures can slow corrosion but are more likely to cause uniform corrosion [8]. Both high and low flow rates can increase certain types of corrosion, while a moderate flow is the least damaging [11]. It is important to understand the compositions, and parameters of geothermal fluid as it can help in knowing whether scaling or corrosion is going to happen. Multiple mechanisms of corrosion and scaling are promoted by geothermal fluid (hydrogen chloride, hydrogen sulfide, iron sulfide, sulfuric acid, carbonates, silica, and metal sulfates) [13-15].

In general, the principle of geothermal power plants includes wells drilled into the earth to pump steam or hot water to the surface and the reinjection to earth [16]. The steam supply for generator power was taken from the two-phase zones and the deep liquid reservoir. Fig. 1 presents the power station schematic diagram [17]. Separator stations are utilized to separate steam and water (also called brine) from the two-phase fluid. The mixture fluid enters the separator through a spiral inlet. As the fluid rotates, the water with higher densitywill move outward and downwards while the steam with lower density will move inward and upward. The steam produced powers the turbines. The steam is cooled and condenses into water, where it is pumped back into the ground through the injection well. The pipeline system in power plant Wayang Windu station can be categorized into four: the two-phase pipeline, the steam pipeline, the brine pipeline, and the condensate pipeline [18]. The main two-phase pipelines from the production wells to the separator are 36 inches carbon steel pipe. The steam pipeline from the separator the power station is 40 inches carbon steel pipe with an approximate distance of 1 km. The brine pipeline from the separator to the injection well is 30 inches carbon steel pipe with an approximate distance of 8 km. The condensate pipeline from the power station to the injection well is 16 inches carbon steel pipe [18].

In this study, we present observations and analyses related to internal corrosion in condensate pipes in geothermal power plants. In this regard, we have requested pipe pieces and condensate fluid samples from the company Geothermal Power Plants for analysis. The analysis conducted aims to find and obtain information on the causes of the corrosion internal on the condensate pipeline, provide an overview of the corrosion mechanism that occurs in the pipe, prevents, overcome, and provide recommendations to avoid the same failure in the future.

## 2. Materials and Methods

The location of internal corrosion in the geothermal power plant system occurs in the condensate pipeline as in Fig 1. The object material used in this research is the condensate pipe from the power station to the injection well as shown in Fig 2. Technical data from condensate pipes are as follows; pipe material: carbon steel, having an outer diameter of 16 inches (406.4 mm) with an original wall thickness of 17 mm. while operational data: flow rate around 0.9 m/s; operation temperature of 40-50 oC, working pressure 2-10 bar, DO values between 3.4 ppm, and pH <5. This specimen was removed from a condensate pipeline after 10 years of operation. The saturation of water for calcium carbonate of the condensate fluid from the condensate pipeline was sampled and measured using the Langelier Saturation Index (LSI). The observation and failure analysis was carried out by visual and dimensional examination, chemical composition testing, macroscopic, and microscopic examination, Scanning Electron Microscope examination with Energy Dispersed Spectrometer (JEOL JSM-6390A). Deposits in pipes are collected and grind and then analyzed by X-Ray Diffraction (Shimadzu XRD 7000). The quality of the condensate fluid and their tendencies were determined by the Langelier Saturation Index (LSI) method. Also, the corrosion rate of the pipe was simulated by condensate fluid by using a corrosion measurement system (Tafel Polarization-Gamry G750). The measurement of the corrosion rate of the specimen in the condensate media was made close to the field parameter conditions (operating temperature 45 $^{o}$C: flow rate 0.9 m/s; at pH <5), and according to ASTM-G5 standards.

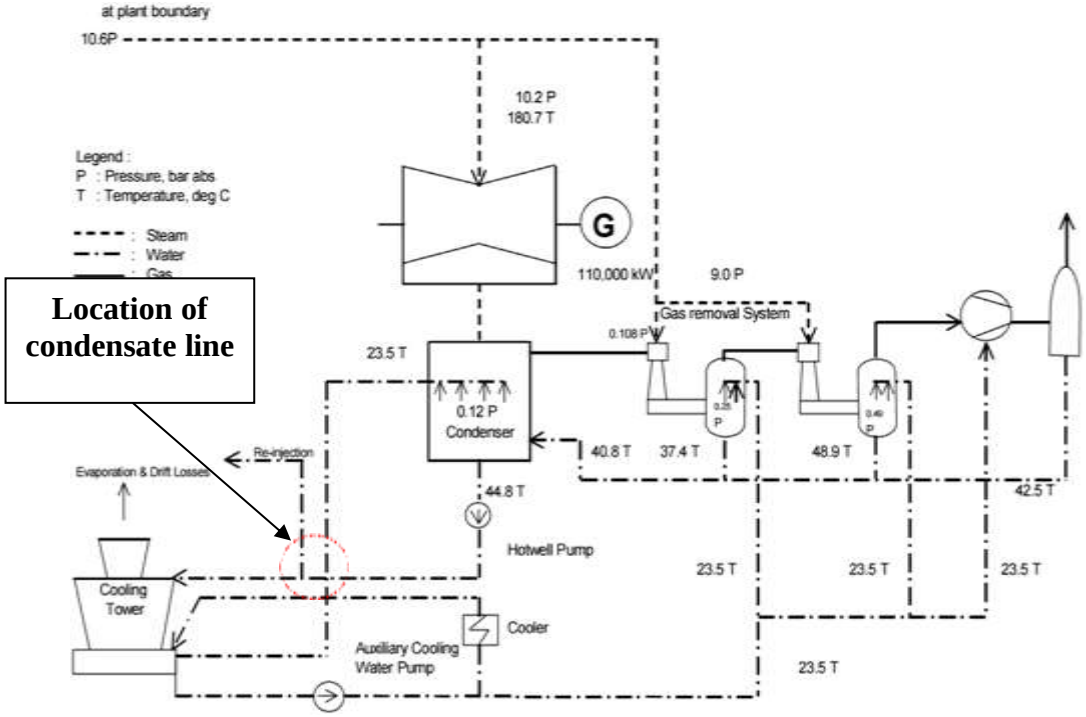


**Fig. 1 - Power station schematic diagram [17]**

**Fig. 2 - A sample cut of the pipe from the condensate pipeline**

## 3. Results and Discussions

### 3.1 Visual Inspection

The first inspection is a visual and dimensional examination. Based on visual observations on the surface area in the pipe, there is visible evenly distributed corrosion on the entire surface. The damage is evident on the internal pipe surface especially at the 6 o'clock position where thewall thickness is found to be thinner than the other sides as shown in Fig. 3. There is a fairly thick deposit at the position at 6 o'clock which is predicted the results of the residual deposition of fluid. The results of the thickness measurement cut-cross section and longitudinal direction are shown in Table 1.

Fig. 3 shows a severe reduction in the thickness of 16-in diameter carbon-steel pipes with an original wall thickness of 17 mm. This specimen was removed from a condensate pipeline after 10 years of operation. The wall-thickness reduced to 42% at the bottom section of the pipe as shown in Fig. 3 and Fig. 4, resulting in a final wall thickness of about 9.86 mm. Also, the thickness reduction of the condensate pipe is found in the longitudinal direction as shown in Fig 4.

The particles in the condensate fluid scratch the internal tube surface, commonly known as a form of erosion-corrosion, and this finding is similar to Fei-Jun, et al. [19] and Yunan, et al. [20] research. The erosion of deposits in solution is estimated to cause non-uniform tube thickness. Erosion usually occurs in pipelines with high flow rates and the presence of insoluble particles [21]. Based on data flow rates on the condensate line (about 0.9 m/s) and referring to the PHCC NSPC-2016 standards, erosion tends to occur. In non-corrosion fluids which have velocity under 0.3 m/s tend to form a scale, and for velocity around 0.3 m/s to 0.9 m/s form uniform corrosion. Meanwhile at above 0.9 m/s of velocity will cause erosion or cavitation corrosion [22]. Increasing the number of insoluble particles in the condensate flow can reduce the thickness of the tube and in turn, cause damage. Increasing the particle speed exponentially increases the rate of erosion [23]. Also, overcoming angles, size, and particles play an important role in surface erosion [24-27].

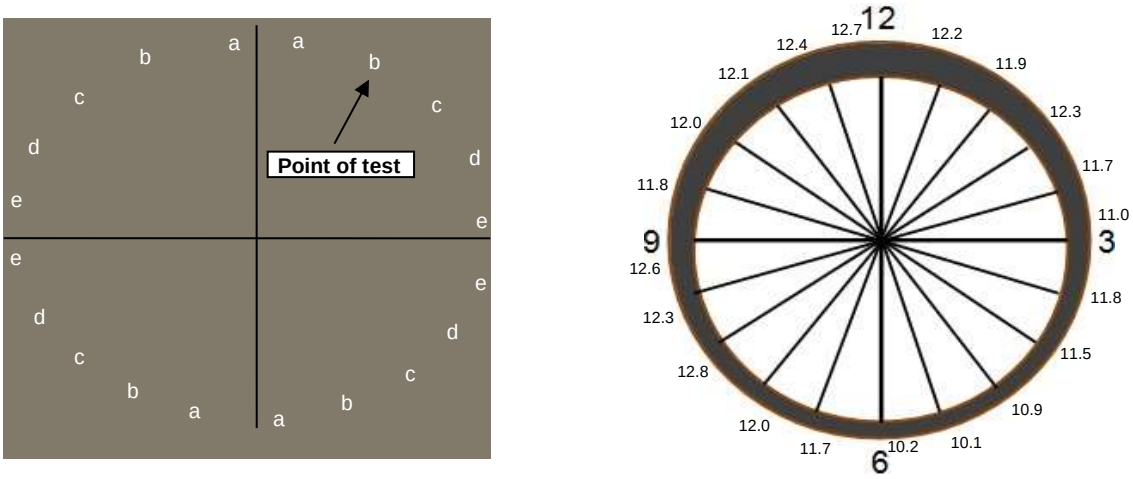


**Fig. 3 - The schematic wall thickness of the pipe (cross-section direction)**

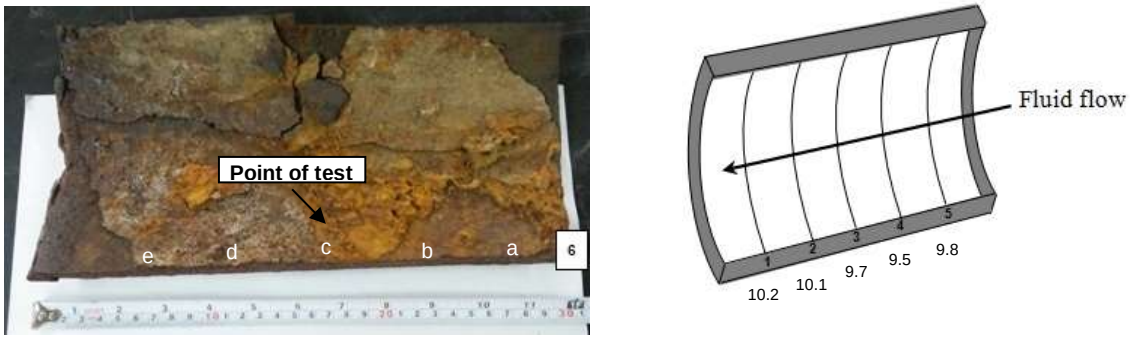


**Fig. 4 - The schematic wall thickness of the pipe (longitudinal direction)**

**Table 1 - The results of the wall thickness of pipe condensate**

| Position (point of test) | Wall Thickness (mm) | | | | |
|---|---|---|---|---|---|
| | Cross-section direction | | | | Longitudinal Direction (6 o'clock) |
| | 3 - 6 | 6 - 9 | 9 - 12 | 12 - 3 | |
| a | 10.2 | 11.7 | 12.7 | 12.2 | 10.2 |
| d | 10.1 | 12 | 12.4 | 11.9 | 10.1 |
| c | 10.9 | 12.8 | 12.1 | 12.3 | 9.7 |
| d | 11.5 | 12.3 | 12 | 11.7 | 9.5 |
| e | 11.8 | 12.6 | 11.8 | 11 | 9.8 |
| **Average** | **10.9** | **12.28** | **12.2** | **11.82** | **9.86** |

## 3.2 Chemical Composition and Microstructures

The chemical composition analysis of the pipe was performed by using spectroscopy, and the result of the chemical composition of these was compared to API 5L Grade B [28] as shown in Table 2. The measurements indicated trends similar to the API 5L grade B. The specimens of damaged pipes were longitudinal-sectioned, mounted, and polished for microstructural analysis. The result of the photomicrograph of pipes is shown in Fig. 5. The damaged pipe contained ferrite grains (bright area) and nodules of pearlite structures (dark area). From Fig. 5, it can be seen that the dominant phase is the ferrite phase (75%), while the pearlite phase is around 25%.

**Table 2 - The result of the chemical composition of the pipe**

| Name | Element (% wt.) | | | | | | | | | | |
|---|---|---|---|---|---|---|---|---|---|---|---|
| | Fe | C | Cr | Ni | Mn | Mo | Al | Si | Cu | S | P |
| Pipe | Balance | 0.0894 | 0.0095 | 0.0155 | 0.9934 | 0.0077 | 0.0273 | 0.2353 | 0.0078 | 0.0044 | 0.0178 |
| API 5L Gr B | Balance | 0.22 max | - | - | 1.28 | - | - | 0.45 | - | 0.03 | 0.03 |

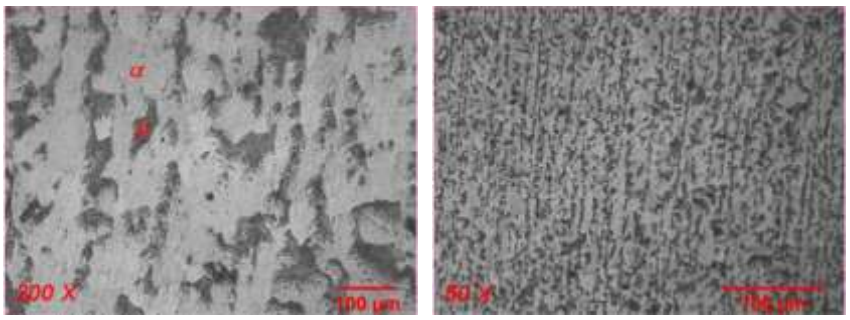


**Fig. 5 - The microstructure of the specimen**

## 3.3 Parameter of Fluid Quality

The Langelier Saturation Index (LSI) obtained from the following expression [6]:

$$LSI = pH - pHS \quad (1)$$

Where pH is the actual pH of the water, and pHS is the pH of saturation. Water at the equilibrium neither dissolves nor precipitates calcium carbonate, so it is then characterized by its saturation pH, called pHS. This is determined using:

$$pHS = (9.3 + A + B) - (C + D) \quad (2)$$

where A, B, C, and D are coefficients that are determined by following:

$$A = (\log [TDS] - 1)/10 \quad (3)$$

$$B = -13.12 \times \log ({}^{o}C + 273) + 34.55 \quad (4)$$

$$C = \log (Ca^{+2}) - 0.4 \quad (5)$$

$$D = \log (Alk) \quad (6)$$

In the above equations, TDS is the total dissolved solids, expressed in ppm; $Ca^{2+}$ is the concentration of Ca (II) ions expressed as $CaCO_3$, in ppm; and Alk is the total alkalinity given in the equalivalent $CaCO_3$ and expressed in ppm. To determine the water indices, the samples of water condensate were used using standard methods and the water quality parameters such as conductivity, temperature, dissolved oxygen (DO), total dissolved solids (TDS), pH, alkalinity, and calcium hardness were measured. The results of condensate fluid quality in condensate pipelines are shown in Table 3.

**Table 3 - The results of the water quality of the condensate pipeline**

| $Ca^{+2}$ Hardness | Total Alkalinity | DO ( mg/L ) | TDS (mg/L) | Conductivity (uS/cm) | Salinity (‰) | pH | Temp. °C |
|---|---|---|---|---|---|---|---|
| 1 | 3.7 | 5.45 | 133 | 278 | 0.13 | 4.3 | 45.2 |

According to the results of chemical analysis in the Table 3, the Langelier Saturation Index (LSI) at 45.2 °C is obtained negative (-6.6). Therefore, the quality of the fluid at the condensate pipeline system is categorized as tending to be corrosive.

## 3.4 The Corrosion Rate of the Pipe

The corrosion rate of the carbon steel pipeline speciment was measured using a three-electrode cell with a saturated calomel electrode (SCE) as the reference electrode. To simulate the actual condition of corrosion process, the water condensate from the condensate line was used as the electrolyte. Fig. 6 shows the polarization diagram (Tafel diagram) for the carbon steel condensate pipeline from which the corrosion rate, given in steady-state curret density $i_{corr}$ ($\mu A/cm^2$), can be determined. In general engineering practice, corrosion rate (CR) expressed in the form of the penetration per unit time (mm/year and mpy) is commonly used and the corrosion rate can be determined by substituting $i_{corr}$, taken from Tafel diagram, to the following equations [3]:

$$CR = 0.129 \frac{i_{corr} \cdot M}{D} \quad (7)$$

The results of the corrosion rate calculation of pipe material are 18.62 $\mu A/cm^2$ or equivalent to 0.58 mm/year (23 mpy). Based on NACE SP0775 standards [29], the corrosion of pipes in condensate lines is categorized into severe categories, as shown in Table 4.

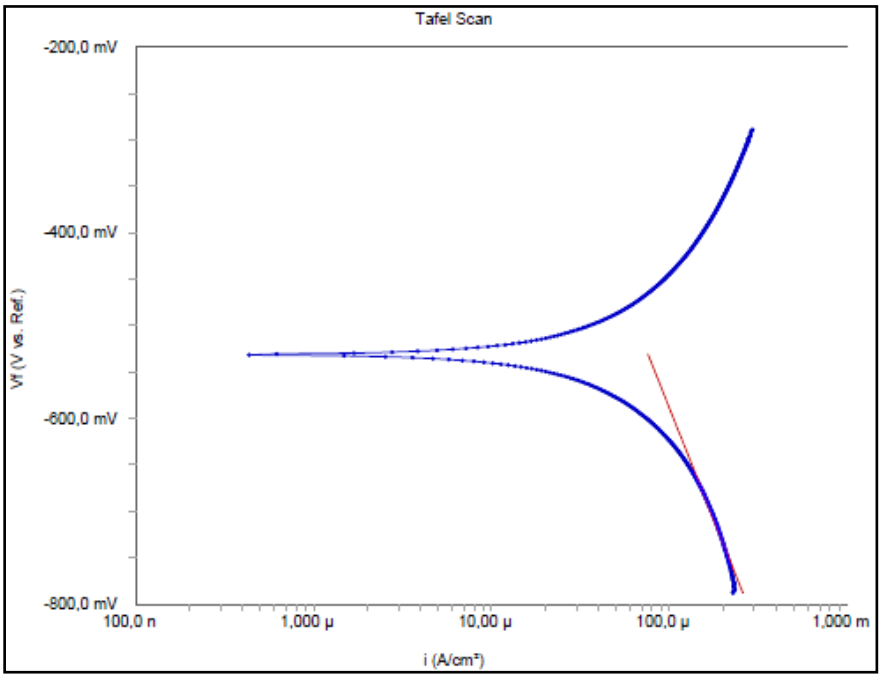


**Fig. 6 - Polarization curves of pipe in the condensate line**

**Table 4 - Qualitative Categorization of Carbon Steel Corrosion Rates for Oil Production Systems [29]**

| Average Corrosion Rate | | |
|---|---|---|
| Category | Mm/y | mpy |
| Low | < 0.025 | < 1.0 |

| | | |
|---|---|---|
| Moderate | 0.025 – 0.12 | 1.0 – 4.9 |
| High | 0.13– 0.25 | 5.0 – 10 |
| Severe | > 0.25 | > 10 |

(A) mm/y = millimeters per year
(B) mpy = mils per year

## 3.5 SEM-EDS

Fig. 7 shows the surface micro-morphology of the deposit separated from the bottom pipes (6 o'clock position). EDS results of the deposit are shown in Fig. 8 with the element containing in Table 5. The deposit mainly consists of calcium, silicon, aluminium, and oxygen. From Fig. 4 and Fig. 7 shows the deposit distribution on the inside wall of steel tube pipes caused by the action of gravity. We find thet erosion is distributed around the tube in the lengthwise direction at bottom side pipes and the erosion zone leads to a longitudinal direction as the measurement of the wall thickness of the pipe in Table 1.

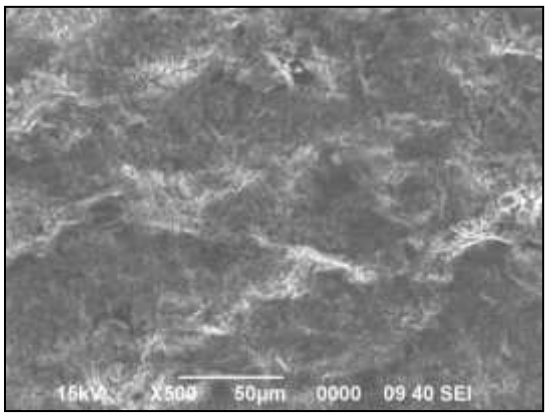


**Fig. 7 - Morphology of deposit at 6 o'clock position**

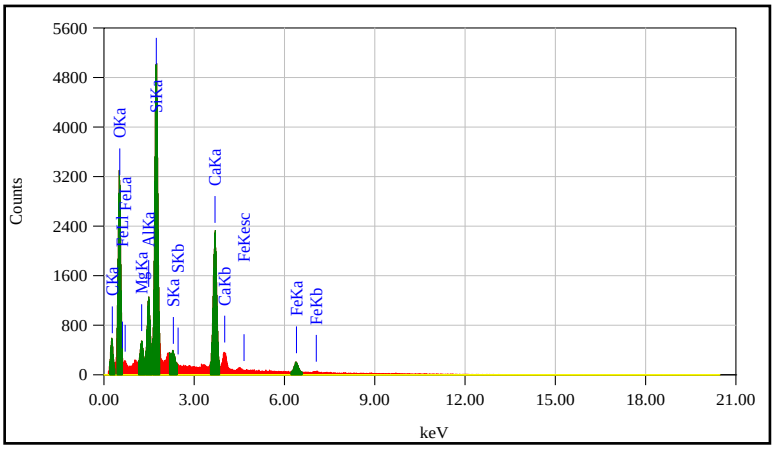


**Fig. 8 - The results of EDS for deposit at 6 o'clock position**

**Table 5 - The element of deposit at 6 o'clock position**

| Element | C | O | Mg | Al | Si | P | S | Ca | Fe |
|---|---|---|---|---|---|---|---|---|---|
| Mass (% wt.) | 9.63 | 37.44 | 1.51 | 4.12 | 18.63 | 0.00 | 0.76 | 21.87 | 6.03 |

Fig. 9 is the microscopic morphology of the deposit at the 3 o'clock positions imaged by SEM. In the circumferential direction is a brown dark-coloured deposit formed from the remaining of the deposit products in the internal wall pipes. The results of EDS demonstrate that the deposit mainly consists of iron, oxygen, silicon, aluminium, and calcium, shown in Fig. 10 and Table 6. It seems clear that the elemental content of calcium and silicon in the deposit at the 6 o'clock position is much higher than in the 3 o'clock position. This reinforces the results of the measurement of the pipe-wall thickness on the inside bottom of the pipe which is thinner due to particle erosion and by the action of gravity.

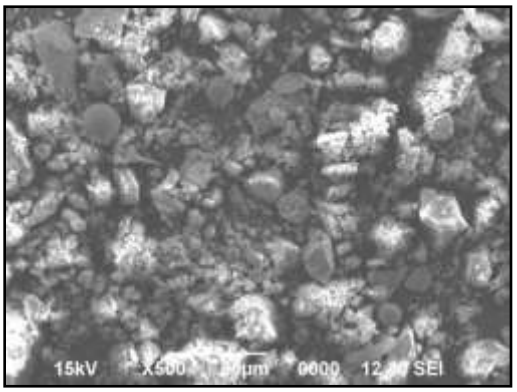


**Fig. 9 - Morphology of deposit on the inner at 3 o'clock position**

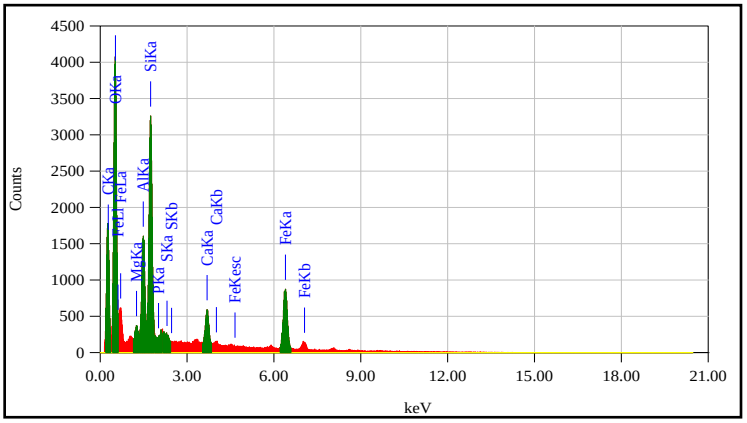


**Fig. 10 - The EDS of deposit on the inner at 3 o'clock position**

**Table 6 - The element of deposit at 3 o'clock position**

| Element | C | O | Mg | Al | Si | P | S | Ca | Fe |
|---|---|---|---|---|---|---|---|---|---|
| Mass (% wt.) | 23.56 | 28.59 | 0.82 | 4.96 | 10.72 | 0.00 | 0.27 | 3.83 | 27.26 |

## 3.6 X-Ray Diffraction

The results of X-ray diffraction patterns from deposits within the condensate pipe are shown in Fig. 11. The main content of compounds in the sediment consists of Calcium Silicate ($Ca_2SiO_4$), Iron Silicate ($Fe_2SiO_4$), Iron Oxide ($Fe_2O_3$), and Pyrite ($FeS_2$). Silicate may be a substance that contains silicon (Si) and oxygen which present naturally as minerals like quartz, amorphous, and Cristobalite [30]. Silicates are characterized by containing silicate ions $SiO_4^-$ because of the smallest building block. Additionally, most silicates are hard, insoluble in water, and acid and thermally stable [31]. Moreover, silicate compounds exist within the style of amorphous which is soluble in alkali solutions and crystalline form that's none stable [32]. Scaling may be a phenomenon that means that a surface is roofed with solid material within the style of crystals of solid salt, precipitating from aqueous solutions [33]. Scaling may be a problem on surfaces of tanks, pipes, evaporators, and heats exchanger and destroys equipment and reduces the flow through the tube, and also decreases the heat transfer rate within the device [33 & 34]. Removing these scales is one of the foremost difficult challenges in industries; therefore, it often requires the employment of mechanical and/or chemical methods [34].

The presence of hard particles (calcium silicate) causes thinning due to the erosion of particles in the fluid. The test results show that a rapid reduction in thickness can be attributed to erosion caused by hard particles in the condensate liquid under the flow rate and working pressure. Besides calcium silicate, there are also iron silicate and iron oxide. Iron silicates are soft compared to calcium silicates ($Ca_2SiO_4$) which are hard [35]; therefore, it's easier to get rid of iron silicates from the equipment surface [36]. Furthermore, iron silicate doesn't bind to the metal surface and don't destroy carbon steel, while calcium silicate, which sorts of hard scaling on the surface, damage the equipment. Silicate scaling results not only reduce quality within the power products but also reduces equipment life and system operations in power plants [37]. Preventing silica scaling on equipment surfaces is one of the foremost difficult challenges, and infrequently requires the employment of mechanical and/or chemical methods [38].

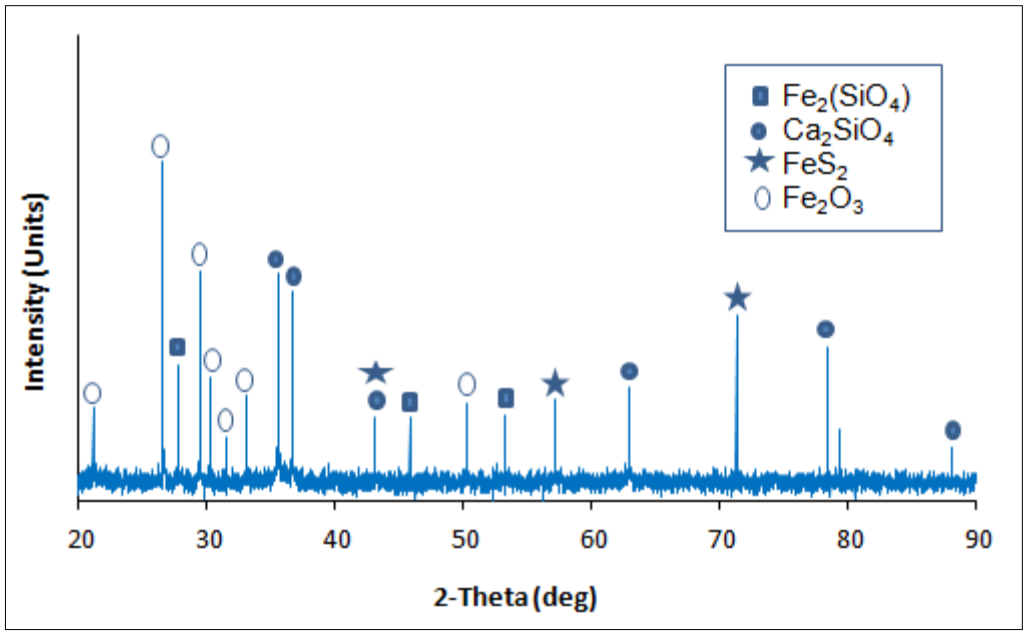


**Fig. 11 - The results of X-ray diffraction patterns from deposits**

## 4 Conclusions

A damaged pipe of condensate pipeline taken from a power plant was investigated in this study to determine the root cause of failure. The internal corrosion was found on the bottom of the pipe, and its wall thickness was thinner than the other inside. From the results of observation and testing, internal corrosion in the condensate line is strongly suspected to occur due to erosion-corrosion. Erosion corrosion is caused by insoluble and hard particles in the condensate fluid. The results of X-Ray Diffraction found the presence of calcium-silicate compounds in the sediment that is suspected to be the cause of erosion particles. The reduction of the thickness of the bottom pipe wall and occurs in longitudinal directions the alleged damage to the pipe due to sediment erosion-corrosion. The presence of hard compounds and differential oxygen can accelerate the process of corrosion so that the corrosion rate in condensate pipelines was a category to the severe category based on NACE SP0775 standards.

## Acknowledgements

The authors gratefully thank Star Energy Geothermal Ltd-Indonesia for providing the materials in conducting this research. The author also would like to thank the Reseach Center for Metallurgy and Materials for laboratory facilities supporting.

## References

[1] Fauzi, A. (2015). Geothermal Resources and Reserves in Indonesia: An Updated Revision. Geoth. Energ. Sci., 3, 1–6

[2] Einar Gunnlaugsson, Halldor Armannsson, Sverrir Thorhallsson and Benedikt Steingrímsson. (2014). Problems In Geothermal Operation – Scaling And Corrosion. Presented at "Short Course VI on Utilization of Low- and Medium-Enthalpy Geothermal Resources and Financial Aspects of Utilization", organized by UNU-GTP and LaGeo, in Santa Tecla, El Salvador, March 23-29, 2014

[3] Jones, D. A. (1996). Principles and prevention of corrosion. New York:Prentice-Hall Inc

[4] Borrmann, T.& Johnston, H, J. (2017). Transforming Silica into Silicate – Pilot Scale Removal of Problematic Silica from Geothermal Brine. GRC Transactions, Vol. 41

[5] Sadiq, J. Z., Blair, C. W., & Chris, M. (2014). Silica scaling in geothermal heat exchangers and its impact on pressure drop and performance: Wairakei binary plant- New Zealand, Geothermics, vol. 51, 445–459

[6] Roberge, P. R. (2008). Corrosion engineering: principles and practice. New York: McGraw-Hill

[7] Bennett, P. B. (1992). Control of environmental variables in water. Resirculating system. Metal Handbook Ninth Edition, New York, USA: Calgon Corporation

[8] Revie, R. W. & Uhliq, H. H. (2008). Corrosion and Corrosion Control: An Introduction to Corrosion Science and Engineering. 4th Edition. Canada, USA: John Wiley & Sons

[9] Mansoori, H., Brown, B., Young, D., Nesic, S. & Singer, M. (2019). Effect of Calcium Ions and CaCO3 Scale on the CO2 Corrosion Mechanism of Mild Steel. Corrosion Conference & Expo 2019, NACE International. Houston, Texas, paper 13000
[10] Royani, A., Prifiharni, S., Priyotomo, G., Triwardono, J., & Sundjono. (2019). Corrosion Performance of Carbon Steel in Pipe Simulation Test for Cooling Water Systems. Metalurgi, Vol. 2, 49 – 60
[11] Tobon, A.C., Cruz, M.D., Aguilar, M.A., & Gonzalez, J.L. (2015). Effect of flow rate on the corrosion products formed on traditional and new generation API 5L X-70 in a sour brine environment. Int. J. Electrochem. Sci.,vol. 10, 2904-2920
[12] Nagalakshmi, T., & Sivasakthi, A. (2019). Corrosion Control, Prevention and Mitigation in Oil & Gas Industry. International Journal of Innovative Technology and Exploring Engineering (IJITEE), Vol. 9 (2), 1568-1572
[13] Einar, G., Halldor, A., Sverrir, T. & Benedikt, S. (2014). Problems in Geothermal Operation - Scaling and Corrosion. Presented at "Short Course VI on Utilization of Low- and Medium-Enthalpy Geothermal Resources and Financial Aspects of Utilization", organized by UNU-GTP and LaGeo, in Santa Tecla, El Salvador, March 23-29, 2014
[14] Andritsos, N., Karabelas, A.J. & Koutsoukos, P.G. (2014). Scale Formation in Geothermal Plants. International Summer School on Direct Application of Geothermal Energy. 179-189
[15] Barja, A. (2014). A Review of Mineral Scaling and Its Mechanisms in Hverageroi Geothermal District Heating System. Master Thesis of Science in Energy Engineering - Iceland School of Energy. School of Science and Engineering - Reykjavík University
[16] Dipippo, R. 2012. Geothermal Power Plants:principles, Applications, Case Studies and Environmentals Impact. Third Edition. Elsevier
[17] Hiroshi Murakami, Yoshifumi Kato, Nobuo Akutsu. (2000). Construction Of The Largest Geothermal Power Plant For Wayang Windu Project, Indonesia. Proceedings World Geothermal Congress 2000. Kyushu - Tohoku, Japan, May 28 - June 10, 2000
[18] Munggang, H. P. & Purwakusumah, A., (2015). Fifteen Years (Mid-Life Time) of Wayang Windu Geothermal Power Station Unit-1: An Operational Review. Proceedings World Geothermal Congress 2015. Melbourne, Australia, 19-25 April 2015
[19] Fei-Jun, C., Cheng, Y., Zhen-Guo, Y. (2014). Failure analysis on abnormal wall thinning of heat-transfer titanium tubes of condensers in nuclear power plant Part I: Corrosion and wear. Engineering Failure Analysis 37, 29–41
[20] Yunan, W., Tianpeng, W., & Mingcheng, S. (2018). Failure Analysis on Leakage of Brass Condenser Tube in Thermal Power Plant. IOP Conf. Series: Materials Science and Engineering 439, 052005
[21] Mahdi, E., Rauf, A., Ghani, S., El-Noamany, A. & Pakari, A. (2013). Erosion-Corrosion Behavior and Failure Analysis of Offshore Steel Tubular Joint. Int. J. Electrochem. Sci., Vol. 8, 7187 – 7210
[22] Singley, J.E., Beaudet, B.A & Markey, P.H (1984). Corrosion Manual for Internal Corrosion of Water Distribution Systems, U.S. Environmental Protection Agency, section 3.3, pp.11–12
[23] Malka, R., Nesic,S. & Daniel A. G. (2006). Erosion Corrosion and Synergistic Effects in Disturbed Liquid-Particle Flow. Corrosion NACExpo 2006, NACE International. Houston, Texas, paper 06594
[24] Paul, O. & Adel, M. A. M. (2014). Erosion-Corrosion in Oil and Gas Industry: A Review. International Journal of Metallurgical & Materials Science and Engineering (IJMMSE), Vol. 4, (3), 7-28
[25] Sudhagar, M., Ragul, M., Nandhini, M., Priyadharshini, M., & Mathi, R. (2017). A Review on Tube Failure Analysing and Improving Condenser Performance. International Journal for Research in Applied Science & Engineering Technology (IJRASET), Vol. 5 (4)
[26] Kolawole, F.O., Kolawole, S.K., Agunsoye, J.O., Adebisi, J.A., Bello, S.A., & Hassan,S.B. (2018). Mitigation of Corrosion Problems in API 5L Steel Pipeline – A Review. J. Mater. Environ. Sci.,Vol. 9 (8), 2397-2410
[27] Groysman, A. (2017). Corrosion problems and solutions in oil, gas, refining and petrochemical industry. Koroze a ochrana materialu, Vol. 61 (3), 100-117
[28] (2010). API 5L, Line Pipe, American Petroleum Institute
[29] NACE SP0775, (2013). Standard Practice Preparation, Installation, Analysis, and Interpretation of Corrosion Coupons in Oilfield Operations. NACE International: The Corrosion Society
[30] Basu, S. (2011). Crystalline Silicon – Properties and Uses. Croatia: InTech Publisher
[31] Andhika, M., Mariela, H. C., & Simona, R. (2015). Characterization of Silica Precipitation at Geothermal Conditions. Proc. World Geothermal Congress 2015. Melbourne, Australia
[32] Daniela B. H., Einar, G., Ingvi, G., Tomasz, M. S., Caroline, L. P., & Liane G. B. (2018). Understanding amorphous silica scaling under well-constrained conditions inside geothermal pipelines. Geothermics 76, 231-241
[33] Emine, T., & Nadieh, S. (2014). Silica Scale Inhibition in Mechanical Pulping: With Focus on Refinery Process. Bachelor of Science Thesis. Department of Chemical and Biological Engineering - Chalmers University of Technology. Sweden: Gothenburg
[34] Brown, K. (2013). Mineral Scaling In Geothermal Power Production. Geothermal Training Programme, Reports 2013, Number 39. Iceland: United Nations University

[35] Yousuf M. R., Shaik, F., & Nageswara, L. R. (2017). Studies on Scale Deposition in Oil Industries & Their Control. Int. J. for Innovative Research in Sci. & Tech. (IJIRST), Vol. 3(12/ 024), 152-167
[36] Ngothai, Y., Lane, D., Kuncoro, G., Yanagisawa, N., Rose, P., & Pring, A. (2012). Effect of Geothermal Brine Properties on Silica Scaling in Enhanced Geothermal Systems. GRC Transactions, Vol. 36871-880
[37] Sverrir Thorhallsson. (2012). Corrosion in Geothermal Wells And Installations. Presented At "Short Course On Geothermal Development And Geothermal Wells", Organized By Unu-Gtp And Lageo, In Santa Tecla, El Salvador, March 11-17, 2012
[38] Ilman, M. N. & Kusmono. (2013). Analysis of internal corrosion in subsea oil pipeline. Case Studies in Engineering Failure Analysis, 1-18